


Identification of a novel biomarker for pyridoxine-dependent epilepsy: Implications for newborn screening

Michael F. Wempe¹ | Amit Kumar¹ | Vijay Kumar¹ | Yu J. Choi¹ | Michael A. Swanson² | Marisa W. Friederich² | Keith Hyland³ | Wyatt W. Yue⁴ | Johan L. K. Van Hove² | Curtis R. Coughlin II² 

¹School of Pharmacy, Department of Pharmaceutical Sciences, University of Colorado, Aurora, Colorado

²Department of Pediatrics, Section of Clinical Genetics and Metabolism, University of Colorado School of Medicine, Aurora, Colorado

³Medical Neurogenetics Laboratories, LLC, Atlanta, Georgia

⁴Structural Genomics Consortium, Nuffield Department of Clinical Medicine, University of Oxford, Oxford, UK

Correspondence

Michael F. Wempe, School of Pharmacy, Department of Pharmaceutical Sciences, University of Colorado, Anschutz Medical Campus, Aurora, CO 12850 E. Montview Blvd, Rm V20-2105 Aurora, Colorado, 80045, USA.

Email: michael.wempe@ucdenver.edu

Curtis R. Coughlin II, Department of Pediatrics, Section of Clinical Genetics and Metabolism, University of Colorado, School of Medicine, Aurora, CO East 17th Ave, L28-3222 Aurora, Colorado, 80045, USA.

Email: curtis.coughlin@ucdenver.edu

Communicating Editor: Sylvia Stockler-Ipsiroglu

Funding information

Pyridoxine-Dependent Epilepsy Foundation; NIH/NCATS Colorado CTSA, Grant/Award Number: UL1 TR001082

Abstract

Pyridoxine-dependent epilepsy (PDE) is often characterized as an early onset epileptic encephalopathy with dramatic clinical improvement following pyridoxine supplementation. Unfortunately, not all patients present with classic neonatal seizures or respond to an initial pyridoxine trial, which can result in the under diagnosis of this treatable disorder. Restriction of lysine intake and transport is associated with improved neurologic outcomes, although treatment should be started in the first year of life to be effective. Because of the documented diagnostic delay and benefit of early treatment, we aimed to develop a newborn screening method for PDE. Previous studies have demonstrated the accumulation of Δ^1 -piperidine-6-carboxylate and α -amino adipic semialdehyde in individuals with PDE, although these metabolites are unstable at room temperature (RT) limiting their utility for newborn screening. As a result, we sought to identify a biomarker that could be applied to current newborn screening paradigms. We identified a novel metabolite, 6-oxo-pipecolate (6-oxo-PIP), which accumulates in substantial amounts in blood, plasma, urine, and cerebral spinal fluid of individuals with PDE. Using a stable isotope-labeled internal standard, we developed a nonderivatized liquid chromatography tandem mass spectrometry-based method to quantify 6-oxo-PIP. This method replicates the analytical techniques used in many laboratories and could be used with few modifications in newborn screening programs. Furthermore, 6-oxo-PIP was measurable in urine for 4 months even when stored at RT. Herein, we report a novel biomarker for PDE that is stable at RT and can be quantified using current newborn screening techniques.

KEYWORDS

6-hydroxy-pipecolate, 6-oxo-pipecolate, ALDH7A1, alpha amino adipic semialdehyde, pyridoxine-dependent epilepsy

1 | INTRODUCTION

Pyridoxine-dependent epilepsy (PDE) is often characterized as a treatment refractory epileptic encephalopathy with dramatic clinical or electroencephalogram improvement after

pyridoxine supplementation.¹ Many patients achieve adequate seizure control with pyridoxine alone. However, 75% of individuals treated with pyridoxine monotherapy have significant intellectual disability (ID) and developmental delay.^{2,3} The degree of ID does not correlate with age of diagnosis or degree of seizure control, suggesting that the cognitive impairment is not solely a result of epilepsy.

PDE is caused by a deficiency of α -amino adipic semialdehyde (α -AASA) dehydrogenase, and results in the accumulation of α -AASA and Δ^1 -piperidine-6-carboxylate (Δ^1 -P6C), which are considered to be in equilibrium.⁴⁻⁶ There are two lysine oxidation pathways that converge at α -AASA. In the saccharopine pathway, the single polypeptide bifunctional enzyme α -amino adipic semialdehyde synthase (AASS) couples lysine with 2-oxoglutarate to produce saccharopine in the lysine ketoglutarate reductase domain followed by the saccharopine dehydrogenase domain which converts saccharopine to glutamate and α -AASA.⁷ In the pipercolate pathway, L-lysine is converted into Δ^1 -piperidine-2-carboxylate (Δ^1 -P2C) via a yet to be identified enzyme and mechanism, although α -transamination has been proposed.⁸ The brain enzyme Δ^1 -P2C reductase (P2CR) then reduces Δ^1 -P2C to L-pipecolic acid (PIP),⁸⁻¹⁰ which is then oxidized via L-pipecolate oxidase resulting in Δ^1 -P6C.¹¹ Of note, Δ^1 -P6C can be converted backwards into PIP via pyrroline-5-carboxylate reductase.^{12,13} Both the pipercolate pathway and the saccharopine pathway converge at Δ^1 -P6C and α -AASA, and α -AASA is further oxidized to 2-amino adipic acid (AAA) by α -AASA dehydrogenase.^{4,14}

Recent treatment paradigms have attempted to reduce the accumulation of α -AASA and Δ^1 -P6C through a lysine-restricted diet and competitive inhibition of lysine-transport.¹⁵⁻¹⁹ These lysine restriction therapies result in significant reduction of α -AASA/ Δ^1 -P6C and improved cognitive outcome, although treatment must be initiated within the first year of life for optimal developmental outcome.²⁰ Unfortunately, the diagnosis of PDE is often delayed.^{2,21} The delay in diagnosis limits the effectiveness of lysine reduction therapies and is a major contributor to the overall morbidity of the disease.

Recent estimates suggest a disease incidence of approximately 1:60 000 live births.²² This is similar to other diseases that currently undergo newborn screening such as galactosemia (1:50 000 live births) and biotinidase deficiency (1:60 000 live births).^{23,24} Because of the benefit of early treatment, documented long diagnostic delay, and sufficiently high frequency of disease incidence, we sought to develop a newborn screening method for PDE. Previous attempts at newborn screening have documented the unstable nature of α -AASA and Δ^1 -P6C at RT.^{25,26} As a result, we attempted to stabilize α -AASA by derivatization with 2,4-dinitrophenylhydrazine (2,4-DNP), but no reaction

product was observed. The subsequent characterization of various metabolites allowed for the identification of a novel metabolite, 6-oxo-pipecolate (6-oxopiperidine 2 carboxylic acid, 6-oxo-PIP), which accumulates in blood, plasma, urine, and cerebral spinal fluid (CSF) of patients with PDE. This new biomarker is stable at RT and can be quantified using current newborn screening techniques, which would make it amiable for newborn screening.

2 | METHODS

2.1 | Human subjects

Three subjects were recruited via the Inherited Metabolic Disease Clinic at Children's Hospital of Colorado on an Institutional Review Board-approved study (COMIRB #16-0585). Inclusion criteria included PDE due to α -AASA dehydrogenase deficiency documented by biallelic mutations in *ALDH7A1* or elevation of α -AASA/ Δ^1 -P6C. Blood, plasma, and urine samples were obtained from three subjects. A CSF sample was obtained from a fourth subject. A control group consisted of anonymous, discarded plasma, urine, and CSF originally obtained for clinical testing at the chemistry laboratory at the Children's Hospital of Colorado (COMIRB #16-1184). Individual written informed consent was obtained from patients.

2.2 | Chemicals and reagents

Deuterium oxide (D_2O), deuterated sulfuric acid (D_2SO_4), deuterated chloride (DCl), deuterated acetic acid (CH_3CO_2D), deuterated ethanol (CH_3CH_2-OD), deuterated ammonium hydroxide (ND_4OD), L-allysine ethylene acetal (AEA), L-lysine, L-glutamine, AAA, PIP, L-amino acid oxidase from *Crotalus adamanteus* (Type IV), Lysine oxidase from *Trichoderma viride*, Catalase from bovine liver, L-saccharopine, NAD^+ , 2,4-DNP, uridine 5'-diphosphoglucuronic acid trisodium salt, amberlyst-15, and 6-oxo-PIP were purchased from Sigma-Aldrich Chemical Company (St. Louis, Missouri). D,L-2-Amino-1,6-hexanedioic-2,5,5-d₃ (D3-AAA) was acquired from CDN Isotopes (Quebec, Canada), and all other reagents were procured from Fisher Scientific (Pittsburgh, Pennsylvania). Control human plasma, blood, and urine were purchased from Bioreclamation LLC (Westbury, New York). Human liver cytosol, S9 and microsomal subcellular fractions were procured from Xenotech LLC (Kansas City, Kansas).

2.3 | Synthesis of standard material

Standards were synthesized through the deprotection of L-allysine ethylene acetal (AEA). In the Amberlyst method,

AEA (11.4 mg) was dissolved in H₂O (1.0 mL) with 76 mg Amberlyst-15 and stirred for 30 minutes at RT. The liquid was transferred to a new glass vial, the beads were then washed with NH₄OH (2 × 1.0 mL), and the contents combined as previously described.²⁷ The material was then concentrated under a N₂ stream and reconstituted with water to a final concentration of 30 mM. In the acid catalyzed method, AEA was similarly dissolved in water and 6 N HCl or H₂SO₄ was added in amounts described in Supporting Information, Table S2, stirred for 30 minutes, and pH-adjusted with NaHCO₃ and diluted with water to a concentration of 20 mM product.

For deuterated experiments in the Amberlyst method, AEA (71 mg) was dissolved in D₂O (2.0 mL) and Amberlyst-15 (721 mg) added and stirred at RT (6 hours) at which point the D₂O was removed and ND₄OD (1.0 mL) added, stirred (15 minutes), and solution removed, and nuclear magnetic resonance (NMR) spectra collected. For deuterated experiments in the acid catalyzed method, AEA was dissolved in D₂O and added either DCl or D₂SO₄ to initiate the reaction, and we then collected the ¹H-NMR and ¹³C-NMR spectra.

2.4 | Aldehyde detection via 2,4-dinitrophenyl hydrazine

The 2,4-DNP reagent procedure was prepared as previously described with minor modifications²⁸; 500 mg of 2,4-DNP was weighed out into a 25 mL Erlenmeyer flask and 4.0 mL water and 11.0 mL ethanol were added and stirred while 2.5 mL H₂SO₄ was added dropwise. The exothermic reaction was cooled with an ice bath. The contents were then allowed to warm to RT and stirred until completely into solution. Two hundred microliter of this solution was added to the analyte solution either during or after the generation from AEA.

2.5 | Hydrogen-1 and Carbon-13 NMR spectroscopy experiments

AEA (10 mg) was dissolved in 700 μL D₂O followed by addition of either 50 μL DCl or D₂SO₄, and immediately transferred to a NMR tube and ¹H and ¹³C spectra collected using a 400 MHz Bruker NMR, Avance III 400; the ¹H-NMR spectra were collected at 400 MHz while the ¹³C-NMR spectra were collected at 100 MHz and the chemical shifts are reported in ppm. Additional NMR experiments were prepared via D₂O and DCl conditions followed by pH adjustment through the addition of NaHCO₃ (1.5 equivalents) to produce Δ¹-P6C.

2.6 | Liquid chromatography tandem mass spectrometry experiments

Lysine metabolites were first analyzed based on previously published liquid chromatography tandem mass spectrometry (LC-MS/MS) methods.^{29,30} As the goal of this study was to replicate current newborn screening modalities, we focused on a nonderivatized MS/MS analytical method.³¹ Samples were analyzed via electrospray ionization in positive ion mode (ESI+) using an Applied Biosystems Sciex 4000 (Applied Biosystems, Foster City, California) equipped with a Shimadzu HPLC (Shimadzu Scientific Instruments, Inc., Columbia, Maryland), and a Leap auto-sampler (LEAP Technologies, Carrboro, North Carolina). Methanol (MeOH): acetonitrile (ACN) 200 μL 1:1 mixture was added to 100 μL of plasma, blood, urine, CSF, or standard materials. Plasma and blood samples were centrifuged at 10 000 rpm and the supernatants used. Urine and CSF samples required no additional processing. The liquid chromatography separation of 10 μL sample was done on two tandem Zorbax-C8 150 × 4.6 mm 5 μm columns with a Zorbax-C8 guard column (Agilent Technologies, Waltham, MA, USA) operated at 40°C with a 0.4 mL/min flow-rate, using the mobile phases A (10 mM NH₄OAc, 0.1% formic acid in H₂O) for 12.0 mM, linear ramp to 95% mobile phase B (1:1 ACN:MeOH) at 16.0 minutes, held for 11.5 minutes, followed by ramping back to A and held for a total run time of 32.0 minutes. Samples were analyzed using the following conditions: (a) ion-spray voltage of 5500 V; (b) temperature, 450°C; (c) collision using nitrogen gas with curtain gas set at 10 and collisionally activated dissociation (CAD) set at 12; (d) ion source gas one (GS1) and two (GS2) were set at 30; (e) entrance potential was set at 10 V; (f) quadrupole one (Q1) and (Q3) were set on unit resolution; (g) dwell time was set at 200 milliseconds. The retention times, mass transitions and other settings are listed in Table S1.

2.7 | Synthesis of standards

The internal standard d3-3,5,5-6-oxopipicolate (D3-oxo-PIP) was synthesized by refluxing D₃-AAA (40 mg, 0.24 mmol) in 20% mono-deuteroacetic acid (CH₃COOD)/D₂O (1.0 mL) at 108°C for 3.5 hours, followed by solvent evaporation under reduced pressure and drying on high vacuum for 1.0 hours, after which deuterated ethanol (CH₃CH₂OD; 10 mL) was added, stirred, and filtered twice. The combined two filtrate solutions were concentrated on reduced pressure and dried on high vacuum (4 hours) resulting in 14 mg deuterated 6-oxo-PIP of >97% purity by NMR and LC-MS/MS analysis.

2.8 | Enzymatic production of lysine metabolism products

To evaluate the products of lysine metabolism through the pipecolate pathway we synthesized the intermediate Δ^1 -P2C enzymatically as follows. Lysine 50 mM with 100 μ L bovine catalase (12.1 mg catalase powder in 1.0 mL phosphate-buffered saline (PBS) buffer pH 7.4) and 50 μ L *T. virida* lysine oxidase (acquired enzyme diluted with 250 μ L water) in 750 μ L PBS were incubated at 37°C for 1 hour, and 100 μ L samples were obtained at 0.5, 2, 5, 10, 15, 30, 45, and 60 minutes, added to 300 μ L 1:1 MeOH:ACN, and analyzed via LC-MS/MS. To identify the reaction product of the saccharopine pathways, recombinant saccharopine dehydrogenase domain of human AASS-SDH was expressed in insect Sf9 cells and purified by chromatography methods (Yue W.W. et al., manuscript in preparation). Stock saccharopine (10 mM; 100 μ L; 1.0 mM final) and NAD⁺ (100 μ L; 1.0 mM final) were added to PBS (790 μ L; pH 7.4), and after preincubation at 37°C for 5 minutes, the reaction was initiated by addition of 10 μ L purified human AASS-SDH and 100 μ L samples taken at 0.5, 5, 10, and 15 minutes, were diluted with 400 μ L 1:1 MeOH:ACN and analyzed by LC-MS/MS.

α -AASA dehydrogenase was expressed in BL21 StarTM (DE3) *Escherichia coli* (Thermo Fisher) cultures transformed with the pET15b vector containing *ALDH7A1*,³² and harvested 3 hours after induction by 1.0 mM IPTG. Expression culture lysate was combined with 2.2 mM NAD⁺ and 0.6 mM Δ^1 -P6C for 5 minutes at 30°C^{22,32,33} and quenched by adding 100 μ L glacial acetic acid to reaction solution (500 μ L).

2.9 | Cytosolic and mitochondrial metabolism of lysine metabolites

Human liver cytosol 100 μ L (10 mg/mL) or S9 fraction 100 μ L (20 mg/mL) and 100 μ L NAD⁺ (1.2 mM final) in 400 μ L PBS pH 7.4 were preincubated at 37°C for 5 minutes, followed by addition of 100 μ L Δ^1 -P6C (100 μ M); 100 μ L samples were taken at 0.5, 5, 20, and 50 minutes, added to 300 μ L 1:1 MeOH:ACN and analyzed by LC-MS/MS. To probe potential phase II metabolism, 100 μ L human liver microsomes (20 mg protein/mL) were similarly incubated with 4.0 mM UDPGA.

Human liver mitochondria were freshly prepared by homogenization of a human liver sample with a Teflon pestle in 5% weight to volume Zheng buffer,³⁴ and after centrifugation at 5600g for 5 minutes, the supernatant was transferred to a centrifuge tube; this procedure was repeated on the resuspended pellet a second time. Both supernatants were combined, centrifuged at 37 500g for 5 minutes, the resulting pellet resuspended in Zheng buffer, homogenized

and similarly pelleted again, and resuspended in 300 μ L Zheng buffer to provide a mitochondrial preparation, with protein concentration determined using the Bio-Rad Protein Assay. To access the mitochondrial matrix, the homogenate was subjected to three freeze-thaw cycles, followed by 2 \times 7 bursts of sonication on ice using a Branson 450 digital sonifier with a 2-in. cup horn at 30% amplitude. Of this mitochondrial preparation 100 μ L was similarly incubated with Δ^1 -P6C and analyzed as above.

2.10 | Biomarker stability studies

In a 4-month stability study, fresh urine samples (400 μ L) from two subjects were aliquoted into 1.5 mL Eppendorf tubes and stored either at RT (22°C \pm 2°C), freezer (−13°C \pm 3°C), or deep freezer (−77°C \pm 3°C) and sampled over 4-months.

2.11 | Computational calculations

Chemical structures were drawn using (ChemDraw Ultra 6.0.1, PerkinElmer Informatics, Cambridge, MA, USA) and z-matrix utilized to perform calculations via Gaussian G98w. Structures were optimized using molecular mechanics and calculations performed at the HF/6-31G level of theory, followed by B3LYP//HF/6-311++G.

3 | RESULTS

3.1 | Identity of the standards made from L-allysine ethylene acetal

Following preparation from AEA by the Amberlyst 15/NH₄OH method, two peaks were noted on LC-MS/MS with t_R = 8.5 minutes and mass transitions 128.2 \rightarrow 82.0, and 55.0 m/z presumed to be Δ^1 -P6C (Figure S1A), and with t_R = 9.0 minutes and mass transitions 146.3 \rightarrow 128.0, 82.1 and 55.1 m/z presumed to be α -AASA (Figure S1B). The relative intensities of these two peaks varied with the catalyst used (Amberlyst-15 vs H₂SO₄ or HCl), time, and the pH of the solution (Table S2). Acid catalyzed deprotection without pH neutralization resulted in a single signal at t_R 9.0 minutes enabling further characterization through DNPH reactivity and NMR spectroscopy.

3.2 | Aldehyde detection via 2,4-dinitrophenyl hydrazine

2,4-DNP reagent was added to positive controls including 4-ethoxybenzaldehyde (3.4 mg; red precipitant), octanal (4.2 mg; yellow precipitant), hexanal (3.8 mg; yellow precipitant), and acetone (5.6 mg; yellow precipitant).

Compounds were prepared in 1.5 mL Eppendorf tubes as 50% ethanol solutions (400 μ L) and 2,4-DNP reagent (200 μ L) was added and mixed. Two different AEA 2,4-DNP reactions were performed with AEA. First, AEA (5.0 mg) was diluted with water (150 μ L) and 50% ethanol (150 μ L). A volume of 200 μ L of the 2,4-DNP reagent (containing sulfuric acid) was immediately added and a chemical reaction was noted with formation of a yellow precipitant, which was characterized by LC-MS/MS to have a mass consistent with 2,4-DNP-AASA adduct (Figure S2A). Next, we allowed the AEA reaction to occur for 1.0 hours followed by 50% ethanol (150 μ L). Once this reaction was completed, 200 μ L of the 2,4-DNP reagent was added without evidence of a chemical reaction (Figure S2B). The reaction was warmed at 37°C and allowed to cool without evidence of solid formation (chemical reaction). This data suggested that the aldehyde, which is present during formation, rapidly cyclized and is no longer present in the final product. To verify this assumption, NMR spectroscopy was performed.

3.3 | Hydrogen-1 and Carbon-13 NMR spectroscopy experiments

^1H and ^{13}C -NMR studies were performed to confirm the identity of the starting material AEA using acid catalyzed deprotection without neutralization, which resulted in a single peak at t_{R} 9.0 minutes. This was initially presumed to be α -AASA but did not react with 2,4-DNP. In the acid catalyzed reaction product of AEA we did not observe an aldehyde $-\text{CH}$ signal around 9 to 11 ppm in the ^1H -NMR, but rather we observed a downfield signal at 8.2 ppm (Figure S3A). We interpreted this signal as the $-\text{CH}$ alkene within Δ^1 -P6C similar to the alkene $-\text{CH}$ signal at 7.7 ppm published for DL- Δ^1 -pyrroline-5-carboxylic acid.³⁵ In addition, the ^{13}C -NMR spectrum shows signals at 80.5 and 80.7 ppm being consistent with the secondary alcohol carbons consistent with 6-hydroxy-pipecolate (piperidine-6-hydroxy-2-carboxylate, 6-OH-PIP) with the 146 parent mass (Figure S3B). Thus, the ^1H -NMR data, ^{13}C -NMR and LC-MS/MS data suggest a mixture of compounds, which co-elutes at t_{R} 9.0 minutes with an apparent 1:2 ratio via LC-MS/MS with respective m/z of 128 and 146 (Figure S4). Despite a number of experimental conditions including the use of a C18, silica, amine, and cyano columns for the LC-MS/MS experiments, we could not separate what we believe is a Δ^1 -P6C/6-OH-PIP mixture.

As noted above, α -AASA and Δ^1 -P6C are in equilibrium although this equilibrium is not well understood.⁵ Previous studies have noted the difficulty in detecting α -AASA, which is supported by our data presented here, and suggested the equilibrium favors Δ^1 -P6C.³⁶ Computational calculations show that the cyclic forms of 6-OH-PIP Cis and

6-OH-PIP Trans are energetically more stable than the linear aldehyde α -AASA by 9.1 and 5.9 kcal/mol (Table S3). Intramolecular cyclization of α -AASA without loss of water to Δ^1 -P6C/6-OH-PIP is an energetically favorable process.

We assigned the identity of the peak at t_{R} 8.5 minutes as most consistent with Δ^2 -piperidine-6-carboxylate (Δ^2 -P6C), based on the mass transition and NMR spectrum, and deuterated experiments, although absence of an authentic standard prevented absolute identification. There was evidence of the Δ^2 -P6C double bond in the ^{13}C -NMR spectra (108.6 and 127.9 ppm) (Figure S5). These signals were not present under DCI or D_2SO_4 conditions. This data also suggests that Δ^2 -P6C is in equilibrium with Δ^1 -P6C, with Δ^2 -P6C forming more under neutral to basic conditions. Δ^2 -P6C can convert back to Δ^1 -P6C but with incorporation of deuterium under D_2O . Thus, the two peaks of observed reaction products correspond to Δ^2 -P6C at t_{R} 8.6 minutes, and a mixture of Δ^1 -P6C and 6-OH-PIP at 9.0 minutes (Figure S6), with the relative amounts a function of the conditions, time, and pH adjustment used to deprotect the acetal.

3.4 | Reaction products and substrates for enzyme activities in the lysine metabolic pathways

Incubation of saccharopine with purified AASS-SDH and NAD^+ resulted in products that on LC-MS/MS were also consistent with Δ^1 -P6C/6-OH-PIP. Incubation of purified α -AASA dehydrogenase with the Δ^1 -P6C/6-OH-PIP mixture without α -AASA readily produced AAA, indicating that this enzyme catalyzes the ring opening and subsequent oxidation of Δ^1 -P6C/6-OH-PIP. Given that 6-OH-PIP has a secondary alcohol, an alternative pathway to AAA could exist by first oxidation of the alcohol of 6-OH-PIP to 6-oxo-PIP, an amide, followed by hydrolytic ring opening to afford AAA. Incubating the Δ^1 -P6C/6-OH-PIP mixture with a fresh purified mitochondrial preparation only afforded AAA, but incubation of Δ^1 -P6C/6-OH-PIP with human liver cytosol and with the S9 fraction in the presence of NAD^+ showed formation of AAA and small amounts of 6-oxo-PIP (Figure S7). Albeit small, the formation of 6-oxo-PIP raises the possibility of a second pathway. To evaluate if the next step the hydrolytic ring opening of 6-oxo-PIP to afford AAA could proceed, we incubated 6-oxo-PIP with human cytosol, human S9, and human plasma (eg, esterase activity) incubations, but none of these experiments showed a conversion of 6-oxo-PIP to AAA.

To generate authentic standards for the pipecolic pathway, incubation of lysine with L-amino acid oxidase and catalase resulted in small amounts of Δ^1 -P2C and, presumably, the hydrated product piperidine-2-hydroxy-

2-carboxylate (P2H2C) (Figure S8). Incubation with lysine oxidase and catalase was far more efficient in producing Δ^1 -P2C and P2H2C.

3.5 | Quantitative LC-MS/MS method of the lysine pathway metabolites

To evaluate the identified metabolites of the lysine pathway, we expanded the analytic LC-MS/MS method to incorporate lysine, glutamine, AAA, PIP, Δ^1 -P2C/P2H2C, Δ^2 -P6C, Δ^1 -P6C/6-OH-PIP, and 6-oxo-PIP (Figure S9). There are two peaks for 6-oxo-PIP representing the enol and keto form. For quantification, deuterated d3-AAA and d3-6-oxo-PIP were used as internal standards. The limit of detection (LOD) for Δ^1 -P6C/6-OH-PIP was 1.0 μ M and the limit of quantitation (LOQ) was 2.0 μ M (Figure S10A). The LOD and LOQ for 6-oxo-PIP were 2.0 mM and 4.0 mM, respectively (Figure S10B). A standard curve between 0.5 and 500 μ M for quantification of Δ^1 -P6C/6-OH-PIP with internal standard d3-AAA had a correlation coefficient >0.99 , and for quantification of 6-oxo-PIP with the internal standard d3-6-oxo-PIP had a correlation coefficient >0.985 .

3.6 | Human subjects

In all blood, plasma, and urine samples of subjects affected with PDE we detected AAA, PIP, Δ^1 -P6C/6-OH-PIP, and 6-oxo-PIP (Figure S11), whereas in samples from 14 control subjects, we only detected AAA and PIP. In two affected subjects, the amount of 6-oxo-PIP in urine was 156.8 μ mol/mg creatinine and 122.2 μ mol/mg creatinine and for Δ^1 -

P6C/6-OH-PIP was 8.5 μ mol/mg creatinine and 7.5 μ mol/mg creatinine. In plasma, the concentration of 6-oxo-PIP was $2.7 \pm 0.1 \mu$ M and $4.1 \pm 0.1 \mu$ M and the concentration of Δ^1 -P6C/6-OH-PIP was $1.1 \pm 0.1 \mu$ M and $3.0 \pm 0.1 \mu$ M for patients 1 and 2, respectively. In CSF from a subject affected with PDE we also identified Δ^2 -P6C and a small but clear peak of Δ^1 -P2C/P2H2C (Figure S12) in addition to Δ^1 -P6C/6-OH-PIP and 6-oxo-PIP. In three control CSF samples, AAA and PIP were observed but Δ^1 -P6C/6-OH-PIP, 6-oxo-PIP, Δ^2 -P6C, and Δ^1 -P2C/P2H2C were absent.

3.7 | Biomarker stability studies

As a primary aim of this research was to evaluate biomarkers suitable for newborn screening, we analyzed blood spots (Whatman 903 Lot #W-041) from two subjects and controls. In blood spots stored at RT, the signal of Δ^1 -P6C/6-OH-PIP rapidly degraded over time, and became undetectable after a few days. In contrast, 6-oxo-PIP was noted in the initial blood spot (Figure 1). A freeze-thaw study and a 4-month stability study was done in urine samples from subjects 1 and 2 (Table S4). The original concentrations of Δ^1 -P6C/6-OH-PIP for subjects 1 and 2 were $16.1 \pm 1.9 \mu$ M and $27.1 \pm 2.0 \mu$ M, respectively. At RT, Δ^1 -P6C/6-OH-PIP degraded within a couple of days with only trace amounts remaining after 2 weeks. When in the freezer or the deep freezer, Δ^1 -P6C/6-OH-PIP decayed moderately. After 126 days, there was a 53% to 64% loss of Δ^1 -P6C/6-OH-PIP at $-13^\circ\text{C} \pm 3^\circ\text{C}$ and 47% to 48% loss at $-77^\circ\text{C} \pm 3^\circ\text{C}$. The initial 6-oxo-PIP concentrations observed in subjects 1 and 2 were $298 \pm 23 \mu$ M and $440 \pm 4 \mu$ M, respectively. 6-oxo-

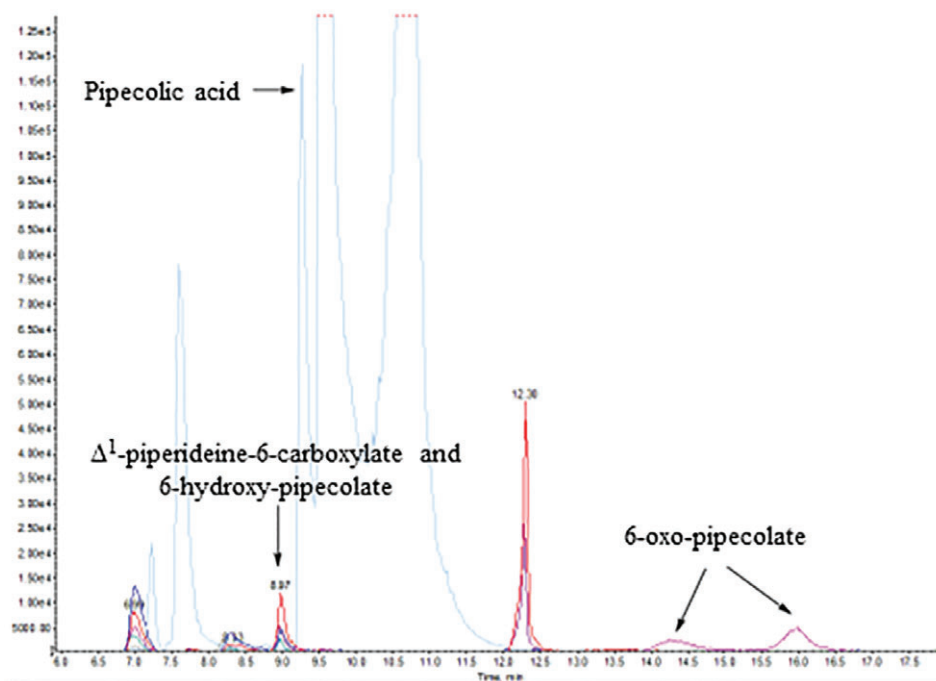


FIGURE 1 Identification of biomarkers in a dried filter paper spot. A dried filter paper (Whatman 903 Lot #W-041) was impregnated with 200 μ L of blood from a patient with pyridoxine-dependent epilepsy. Using a nonderivatized liquid chromatography tandem mass spectrometry method, we identified pipecolic acid, the equilibrium of Δ^1 -piperidine-6-carboxylate and 6-hydroxy-pipecolate (Δ^1 -P6C/6-OH-PIP), and 6-oxo-pipecolate (6-oxo-PIP)

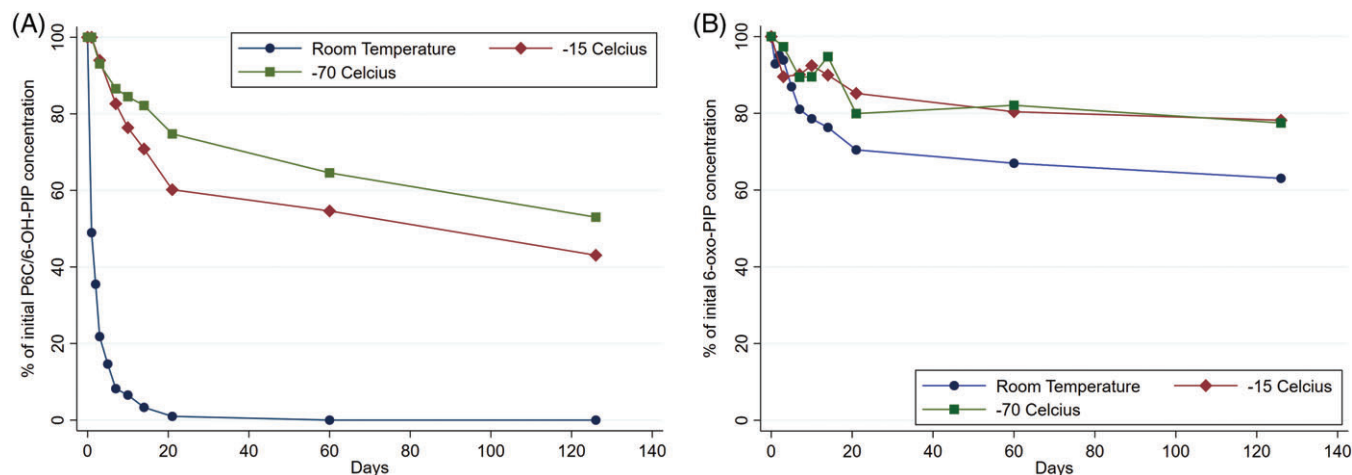
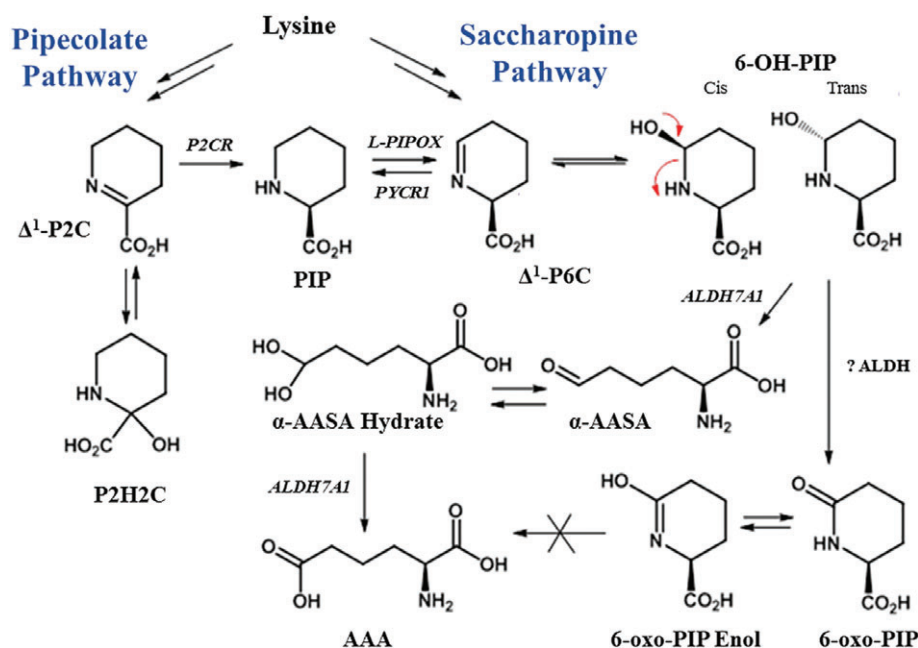


FIGURE 2 Stability study of Δ^1 -piperidine-6-carboxylate and 6-hydroxy-pipecolate (Δ^1 -P6C/6-OH-PIP) and 6-oxo-pipecolate (6-oxo-PIP). A 4-month stability study was performed in urine samples from two subjects with pyridoxine-dependent epilepsy. Δ^1 -P6C/6-OH-PIP and 6-oxo-PIP concentrations were measured in three conditions: room temperature (circle), -15°C (diamond), and -70°C (square). Each sample was measured three times and reported as a mean value; the mean value is represented as the percent of the initial concentration. At room temperature, Δ^1 -P6C/6-OH-PIP degraded quickly (A) whereas 6-oxo-PIP was relatively stable for 126 days (B)

FIGURE 3 Proposed modification to the lysine oxidation pathway. In the revised lysine oxidation pathway, both the pipecolate and the saccharopine pathway converge on the equilibrium of Δ^1 -piperidine-6-carboxylate (Δ^1 -P6C) and 6-hydroxy-pipecolate (6-OH-PIP). The α -aminoadipic semialdehyde (α -AASA) dehydrogenase enzyme acts on this metabolite to generate α -AASA and then 2-amino-adipic acid (AAA). In α -AASA dehydrogenase deficiency, a cytosolic enzyme catalyzed the oxidation of 6-OH-PIP to 6-oxo-pipecolate (6-oxo-PIP). Abbreviations: P2C, Δ^1 -piperidine-2-carboxylate; P2H2C, piperidine-2-hydroxy-2-carboxylate; P2CR, Δ^1 -piperidine-2-carboxylate reductase; PIP, pipecolic acid



PIP showed an initial 20% to 21% decrease within the first 2 weeks regardless of storage temperature with, at room temperature, a slower rate of degradation displaying only a 43% and 33% decrease at 126 days for subjects 1 and 2, respectively. Thus, at RT, 6-oxo-PIP was considerably more stable than Δ^1 -P6C/6-OH-PIP (Figure 2).

4 | DISCUSSION

Herein, we describe a novel biomarker (6-oxo-PIP) for PDE, which has significant implications for newborn screening of

this treatable disease. Previous attempts at newborn screening were limited as the primary biomarkers Δ^1 -P6C and α -AASA degraded rapidly at RT.^{25,26} In our study, 6-oxo-PIP was measurable for up to 4 months in urine samples stored at RT. Stability at RT is essential as the current newborn screen paradigm relies on samples to be collected, dried, and shipped at RT. Using a stable isotope labeled internal standard, we developed a nonderivatized method LC-MS/MS-based method to quantify 6-oxo-PIP in subjects and controls. We suggest that screening for PDE could be added to the current newborn screen paradigm where samples are collected on filter paper cards, dried, and shipped at

RT, and analyzed via nonderivatized MS/MS analytical methods. Further studies are needed to establish the sensitivity and specificity of 6-oxo-PIP for PDE. To our knowledge, 6-oxo-PIP has not been reported in patients with PDE or other defects of lysine metabolism, although it has been identified in *Penicillium chrysogenum*.^{37,38}

The presence of 6-oxo-PIP was suggested by the presence of 6-OH-PIP as an intermediate step between Δ^1 -P6C and α -AASA (Figure 3). 6-OH-PIP represents the cyclization of α -AASA without loss of water and the simple addition of water across the C=N bond in Δ^1 -P6C. Oxidation of the secondary alcohol in 6-OH-PIP results in the formation of 6-oxo-PIP. Our combined NMR, mass spectrometry and DNP reactivity data suggests that a mixture of Δ^1 -P6C/6-OH-PIP exists, although this mixture could not be separated despite the use of multiple analytical methods. We suggest that these two metabolites are in a very rapid equilibrium in any aqueous condition. The initial NMR experiments are consistent with both a double bond and a hydroxyl group. This suggests that both interacting products are present in the original standard and not solely occurring with the analytical mass spectrometry method.

Various mutations in *ALDH7A1* result in the accumulation of Δ^1 -P6C/6-OH-PIP and α -AASA. α -AASA dehydrogenase is present in both mitochondria and cytosol. When Δ^1 -P6C/6-OH-PIP accumulates, it appears to be a substrate of a dehydrogenase using NAD⁺ located in the cytosol, but not in the mitochondria, and resulting in the formation of 6-oxo-PIP. The exact identity of this enzyme still needs to be determined. An alternative possibility includes the formation of pipecolate from the incubated Δ^1 -P6C and a direct oxidation of pipecolate to 6-oxo-PIP. Although this appears less likely, it is not excluded by the data presented in this paper. The 6-oxo-PIP formed cannot be further metabolized to AAA and accumulates in patients with PDE.

Of note, we identified a small but distinct peak of Δ^1 -P2C/P2H2C in the CSF of a single affected subject, which was not identified in blood, plasma, or urine of affected patients. If confirmed, the presence of Δ^1 -P2C/P2H2C may indicate a role for the pipecolate pathway in human brain lysine metabolism. The respective contributions of each pathway cannot be determined from this study, and has been subject of controversy.^{39–41} Further studies are needed to determine which of the many accumulating metabolites contributes to the neurological symptoms of PDE.

5 | CONCLUSION

In summary, we report 6-OH-PIP as an intermediate metabolite between Δ^1 -P6C and α -AASA in lysine oxidation. A

minor cytosolic enzymatic pathway allows oxidation to 6-oxo-PIP. Accumulation of 6-oxo-PIP was identified in the blood, plasma, urine, and CSF of subjects with PDE and represents a novel biomarker. We present an analytical method for quantification of this new biomarker using stable isotope dilution of LC-MS/MS. Unlike previously identified biomarkers for PDE, 6-oxo-PIP was relatively stable at RT. Stability of a biomarker at RT is essential to add screening for PDE into existing newborn screening paradigms. The clinical utility of 6-oxo-PIP will need to be defined in a future study of multiple subjects with PDE.

ACKNOWLEDGMENTS

This work was supported by NIH/NCATS Colorado CTSA (Grant Number UL1 TR001082) and the US-based patient organization: Pyridoxine-Dependent Epilepsy Foundation.

CONFLICTS OF INTEREST

A.K., V.K., Y.J.C., M.A.S., M.W.F., W.W.Y. declare that they have no conflicts of interest. K.H. receives salary and has owner interest in Medical Neurogenetics—a company that performs clinical testing for PDE. M.F.W., J.L.K.V.H. and C.R.C. have a patent application for diagnostic markers for PDE pending.

AUTHOR CONTRIBUTIONS

M.F.W., J.L.K.V.H. and C.R.C. conceived of study design, reviewed data, and drafted the manuscript. M.F.W., A.K., V.K., Y.J.C., M.W.F. and M.A.S. produced, reviewed, and interpreted laboratory data. C.R.C. and K.H. provided patient samples. W.W.Y. and M.A.S. produced specialized purified human enzymes. All authors critically reviewed and contributed to the final manuscript and agreed to be accountable for the final version of the manuscript.

ORCID

Curtis R. Coughlin II  <https://orcid.org/0000-0002-3545-7903>

REFERENCES

- Hunt AD, Stokes J, McCrory WW, Stroud HH. Pyridoxine dependency: report of a case of intractable convulsions in an infant controlled by pyridoxine. *Pediatrics*. 1954;13:140-145.
- Basura GJ, Hagland SP, Wiltse AM, Gospe SM. Clinical features and the management of pyridoxine-dependent and pyridoxine-responsive seizures: review of 63 North American cases submitted to a patient registry. *Eur J Pediatr*. 2009;168:697-704. <https://doi.org/10.1007/s00431-008-0823-x>.

3. Bok LA, Halbertsma FJ, Houterman S, et al. Long-term outcome in pyridoxine-dependent epilepsy. *Dev Med Child Neurol.* 2012; 54:849-854. <https://doi.org/10.1111/j.1469-8749.2012.04347.x>.
4. Mills PB, Struys E, Jakobs C, et al. Mutations in antiquitin in individuals with pyridoxine-dependent seizures. *Nat Med.* 2006;12: 307-309. <https://doi.org/10.1038/nm1366>.
5. Struys EA, Bok LA, Emal D, Houterman S, Willemsen MA, Jakobs C. The measurement of urinary Δ^1 -piperideine-6-carboxylate, the alter ego of α -aminoadipic semialdehyde, in Antiquitin deficiency. *J Inherit Metab Dis.* 2012;35:909-916. <https://doi.org/10.1007/s10545-011-9443-0>.
6. Struys EA, Jakobs C. Metabolism of lysine in alpha-aminoadipic semialdehyde dehydrogenase-deficient fibroblasts: evidence for an alternative pathway of pipercolic acid formation. *FEBS Lett.* 2010; 584:181-186. <https://doi.org/10.1016/j.febslet.2009.11.055>.
7. Vashishtha AK, West AH, Cook PF. Probing the chemical mechanism of saccharopine reductase from *Saccharomyces cerevisiae* using site-directed mutagenesis. *Arch Biochem Biophys.* 2015;584: 98-106. <https://doi.org/10.1016/j.abb.2015.08.023>.
8. Hallen A, Jamie JF, Cooper AJL. Lysine metabolism in mammalian brain: an update on the importance of recent discoveries. *Amino Acids.* 2013;45:1249-1272. <https://doi.org/10.1007/s00726-013-1590-1>.
9. Garweg G, von Rehren D, Hintze U. L-Pipecolate formation in the mammalian brain. Regional distribution of delta1-pyrroline-2-carboxylate reductase activity. *J Neurochem.* 1980;35:616-621.
10. Rothstein M, Miller LL. The conversion of lysine to pipercolic acid in the rat. *J Biol Chem.* 1954;211:851-858.
11. IJlst L, de Kromme I, Oostheim W, Wanders RJ. Molecular cloning and expression of human L-pipecolate oxidase. *Biochem Biophys Res Commun.* 2000;270:1101-1105. <https://doi.org/10.1006/bbrc.2000.2575>.
12. Meng Z, Lou Z, Liu Z, et al. Crystal structure of human pyrroline-5-carboxylate reductase. *J Mol Biol.* 2006;359:1364-1377. <https://doi.org/10.1016/j.jmb.2006.04.053>.
13. Struys EA, Jansen EEW, Salomons GS. Human pyrroline-5-carboxylate reductase (PYCR1) acts on $\Delta(1)$ -piperideine-6-carboxylate generating L-pipecolic acid. *J Inherit Metab Dis.* 2014;37:327-332. <https://doi.org/10.1007/s10545-013-9673-4>.
14. Chan C-L, Wong JWY, Wong C-P, Chan MKL, Fong WP. Human antiquitin: structural and functional studies. *Chem Biol Interact.* 2011;191:165-170. <https://doi.org/10.1016/j.cbi.2010.12.019>.
15. Coughlin CR, van Karnebeek CDM, Al-Hertani W, et al. Triple therapy with pyridoxine, arginine supplementation and dietary lysine restriction in pyridoxine-dependent epilepsy: neurodevelopmental outcome. *Mol Genet Metab.* 2015;116:35-43. <https://doi.org/10.1016/j.ymgme.2015.05.011>.
16. Mahajnah M, Corderio D, Austin V, et al. A prospective case study of the safety and efficacy of lysine-restricted diet and arginine supplementation therapy in a patient with pyridoxine-dependent epilepsy caused by mutations in ALDH7A1. *Pediatr Neurol.* 2016;60: 60-65. <https://doi.org/10.1016/j.pediatrneurol.2016.03.008>.
17. Mercimek-Mahmutoglu S, Cordeiro D, Cruz V, et al. Novel therapy for pyridoxine dependent epilepsy due to ALDH7A1 genetic defect: l-arginine supplementation alternative to lysine-restricted diet. *Eur J Paediatr Neurol.* 2014;18:741-746. <https://doi.org/10.1016/j.ejpn.2014.07.001>.
18. van Karnebeek CDM, Hartmann H, Jaggamantri S, et al. Lysine restricted diet for pyridoxine-dependent epilepsy: first evidence and future trials. *Mol Genet Metab.* 2012;107:335-344. <https://doi.org/10.1016/j.ymgme.2012.09.006>.
19. Yuzyuk T, Thomas A, Viau K, et al. Effect of dietary lysine restriction and arginine supplementation in two patients with pyridoxine-dependent epilepsy. *Mol Genet Metab.* 2016b;118:167-172. <https://doi.org/10.1016/j.ymgme.2016.04.015>.
20. Al Teneiji A, Bruun TUJ, Cordeiro D, et al. Phenotype, biochemical features, genotype and treatment outcome of pyridoxine-dependent epilepsy. *Metab Brain Dis.* 2017;32:443-451. <https://doi.org/10.1007/s11011-016-9933-8>.
21. Falsaperla R, Vari MS, Toldo I, et al. Pyridoxine-dependent epilepsies: an observational study on clinical, diagnostic, therapeutic and prognostic features in a pediatric cohort. *Metab Brain Dis.* 2018;33:261-269. <https://doi.org/10.1007/s11011-017-0150-x>.
22. Coughlin CR, Swanson MA, Spector E, et al. The genotypic spectrum of ALDH7A1 mutations resulting in pyridoxine dependent epilepsy: a common epileptic encephalopathy. *J Inherit Metab Dis.* 2018. <https://doi.org/10.1007/s10545-018-0219-7>.
23. Porta F, Pagliardini V, Celestino I, et al. Neonatal screening for biotinidase deficiency: a 30-year single center experience. *Mol Genet Metab Rep.* 2017;13:80-82. <https://doi.org/10.1016/j.ymgmr.2017.08.005>.
24. Suzuki M, West C, Beutler E. Large-scale molecular screening for galactosemia alleles in a pan-ethnic population. *Hum Genet.* 2001; 109:210-215.
25. Jung S, Tran N-TB, Gospe SM, Hahn SH. Preliminary investigation of the use of newborn dried blood spots for screening pyridoxine-dependent epilepsy by LC-MS/MS. *Mol Genet Metab.* 2013;110:237-240. <https://doi.org/10.1016/j.ymgme.2013.07.017>.
26. Mathew EM, Moorkoth S, Lewis L, Rao P. Biomarker profiling for pyridoxine dependent epilepsy in dried blood spots by HILIC-ESI-MS. *Int J Anal Chem.* 2018;2018:2583215. <https://doi.org/10.1155/2018/2583215>.
27. Sadiilkova K, Gospe SM, Hahn SH. Simultaneous determination of alpha-aminoadipic semialdehyde, piperideine-6-carboxylate and pipercolic acid by LC-MS/MS for pyridoxine-dependent seizures and folinic acid-responsive seizures. *J Neurosci Methods.* 2009; 184:136-141. <https://doi.org/10.1016/j.jneumeth.2009.07.019>.
28. Ruekberg B, Rossoni E. An improved preparation of 2,4-dinitrophenylhydrazine reagent. *J Chem Educ.* 2005;82:1310. <https://doi.org/10.1021/ed082p1310.2>.
29. Struys EA, Jakobs C. α -Aminoadipic semialdehyde is the biomarker for pyridoxine dependent epilepsy caused by α -aminoadipic semialdehyde dehydrogenase deficiency. *Mol Genet Metab.* 2007;91:405. <https://doi.org/10.1016/j.ymgme.2007.04.016>.
30. Yuzyuk T, Liu A, Thomas A, et al. A novel method for simultaneous quantification of alpha-aminoadipic semialdehyde/piperideine-6-carboxylate and pipercolic acid in plasma and urine. *J Chromatogr B Analyt Technol Biomed Life Sci.* 2016a; 1017-1018:145-152. <https://doi.org/10.1016/j.jchromb.2016.02.043>.
31. Nagy K, Takáts Z, Pollreis F, Szabó T, Vékey K. Direct tandem mass spectrometric analysis of amino acids in dried blood spots without chemical derivatization for neonatal screening. *Rapid Commun Mass Spectrom.* 2003;17:983-990. <https://doi.org/10.1002/rcm.1000>.
32. Coulter-Mackie MB, Li A, Lian Q, Struys E, Stockler S, Waters PJ. Overexpression of human antiquitin in *E. coli*:

- enzymatic characterization of twelve ALDH7A1 missense mutations associated with pyridoxine-dependent epilepsy. *Mol Genet Metab.* 2012;106:478-481. <https://doi.org/10.1016/j.ymgme.2012.06.008>.
33. Coulter-Mackie MB, Tiebout S, van Karnebeek C, Stockler S. Overexpression of recombinant human antiquitin in *E. coli*: partial enzyme activity in selected ALDH7A1 missense mutations associated with pyridoxine-dependent epilepsy. *Mol Genet Metab.* 2014;111:462-466. <https://doi.org/10.1016/j.ymgme.2014.02.010>.
34. Zheng XX, Shoffner JM, Voljavec AS, Wallace DC. Evaluation of procedures for assaying oxidative phosphorylation enzyme activities in mitochondrial myopathy muscle biopsies. *Biochim Biophys Acta.* 1990;1019:1-10.
35. Farrant RD, Walker V, Mills GA, Mellor JM, Langley GJ. Pyridoxal phosphate de-activation by pyrroline-5-carboxylic acid. Increased risk of vitamin B6 deficiency and seizures in hyperprolinemia type II. *J Biol Chem.* 2001;276:15107-15116. <https://doi.org/10.1074/jbc.M010860200>.
36. Pena IA, Marques LA, Laranjeira ABA, Yunes JA, Eberlin MN, Arruda P. Simultaneous detection of lysine metabolites by a single LC-MS/MS method: monitoring lysine degradation in mouse plasma. *Springerplus.* 2016;5:172. <https://doi.org/10.1186/s40064-016-1809-1>.
37. Brundidge SP, Gaeta FC, Hook DJ, Sapino C Jr, Elander RP, Morin RB. Association of 6-oxo-piperidine-2-carboxylic acid with penicillin V. Production on *Penicillium chrysogenum* fermentations. *J Antibiot.* 1980;33:1348-1351.
38. Henriksen CM, Nielsen J, Villadsen J. Cyclization of alpha-amino adipic acid into the the delta-lactam 6-oxo-piperidine-2-carboxylic acid by *Penicillium chrysogenum*. *J Antibiot.* 1998; 51:99-106.
39. Pena IA, Marques LA, Laranjeira ABA, et al. Mouse lysine catabolism to amino adipate occurs primarily through the saccharopine pathway; implications for pyridoxine dependent epilepsy (PDE). *Biochim Biophys Acta.* 2017;1863:121-128. <https://doi.org/10.1016/j.bbadis.2016.09.006>.
40. Posset R, Opp S, Struys EA, et al. Understanding cerebral L-lysine metabolism: the role of L-pipecolate metabolism in Gcdh-deficient mice as a model for glutaric aciduria type I. *J Inher Metab Dis.* 2015;38:265-272. <https://doi.org/10.1007/s10545-014-9762-z>.
41. Sauer SW, Opp S, Hoffmann GF, Koeller DM, Okun JG, Kölker S. Therapeutic modulation of cerebral L-lysine metabolism in a mouse model for glutaric aciduria type I. *Brain.* 2011;134: 157-170. <https://doi.org/10.1093/brain/awq269>.

SUPPORTING INFORMATION

Additional supporting information may be found online in the Supporting Information section at the end of the article.

How to cite this article: Wempe MF, Kumar A, Kumar V, et al. Identification of a novel biomarker for pyridoxine-dependent epilepsy: Implications for newborn screening. *J Inher Metab Dis.* 2019;42: 565–574. <https://doi.org/10.1002/jimd.12059>